Computational weld mechanics - Increased accuracy in fatigue assessment, distortion and residual stress analysis

JINCHAO ZHU

Academic Dissertation which, with due permission of the KTH Royal Institute of Technology, is submitted for public defense for the Degree of Doctor of Philosophy on Thursday the 11th November 2022, at 9:00 a.m. in F3, Lindstedtsvägen 26, Stockholm.

Doctoral Thesis in Engineering Mechanics
KTH Royal Institute of Technology
Stockholm, Sweden 2022

ISBN: 978-91-8040-367-2
TRITA-SCI-FOU 2022:50

Printed by: Universitetsservice US-AB, Sweden 2022

Content

Preface

The work in this doctoral thesis has been carried out at the Department of Engineering Mechanics at KTH between August 2017 and November 2022. The work done in this thesis is a part of the DIGFOG project - Smart Digitized Jointing Processes, and VariLight project - Reduced VARIation in the manufacturing processes enabling LIGHTweight welded structures, supported by Sweden's Innovation Agency (VINNOVA) programme for Strategic vehicle research and innovation (FFI).

Some of the work has also been presented and discussed within the commission X, XIII, XV in the International Institute of Welding (IIW) in Shanghai 2017, Bali 2018 and Bratislava 2019. Part of the work has been presented in the 3rd International Conference on Structural Integrity in Madeira 2019 and 9th Edition of the International Conference on Fatigue Design in Senlis 2021. The work in this thesis has been funded by Cargotec Sweden AB Bromma Conquip, SSAB, VINNOVA, CSC and Jernkontoret.

I would like to express my sincere gratitude to my supervisor Professor Zuheir Barsoum and co-supervisors Dr Mansoor Khurshid and Dr Rami Mansoor for their continued support, encouragement, and guidance throughout the work. Associate Professor Imad Barsoum at Khalifa University, Mr. Martin Edgren at KTH, Mr. Hasse Olsson retired from Volvo Construction Equipment, Associate Professor Peter Hammersberg at Chalmers, Mr. Per Lundin at Stresstech Oy and Mr. Joakim Hedegård at Swerim AB are highly acknowledged for their discussions during the projects. I would also like to thank my friends and colleagues at the Department of Engineering Mechanics for providing a nice working environment appreciated.

I am forever grateful to my parents Jiaming and Yiqian and family members for their unconditional love and support. Last, to my grandfather Zhikai, in loving memory.

Stockholm, August 2022

Jinchao Zhu

Abstract

This thesis work is concerned with the mechanical response of welded steel structures, which are distortions, residual stresses, and fatigue. The accuracy of fatigue assessment, distortion and residual stress analysis using Computational weld mechanics (CWM) is focused. The following studies are performed; welding simulations of residual stresses and distortions, weld quality estimation, evaluation of local stress-based fatigue strength assessment methods.

The following CWM methods: thermo-elastic-plastic, inherent strain (local-global), and sub structuring have been implemented both on T-type fillet weld and butt weld specimens to estimate angular distortion and residual stresses. In regard to large welded structures, the CWM methods using lumping method, together with prescribed temperature method, is implemented on a welded box structures to estimate welding residual stress state. The welding distortion analysis has been carried out on a large full scale beam structure experimentally and numerically using CWM techniques such as the inherent strain (local–global) method and the shrinkage method, together with the lumping approach. The accuracy of CWM methods is studied, and improvements are proposed.

A probabilistic model is proposed to estimate the probability of a targeted weld penetration depth. The uncertain process parameters are voltage, current, travel speed, and torch travel angle which were studied based on an experimental investigation. The weld penetration depth is evaluated from macrographs using a digital tool developed in MatLab. The epistemic measurement uncertainty related to this evaluation is quantified and incorporated in the probabilistic model.

Monte Carlo simulation is implemented to consider the weld geometry variations in the ENS methods. The stochastic variability in toe radius, toe angle and leg length are considered. The influence of weld geometry variations on the ENS methods using deterministic and stochastic SCF distribution is assessed.

The Hot Spot Stress (HSS), 1-mm stress (OM), Theory of Critical Distances (TCD), Stress Averaging (SA), and Effective Notch Stress (ENS) methods are evaluated for cover plates and T-joints subjected to axial and bending loading, in terms of accuracy and reliability. The evaluation is based on fatigue test data extracted from the literature and carried out in this study. The fatigue design curves applicable for T-joints under bending are discussed, which can be used in the TCD method and SA method.

The studies above contribute to increasing the accuracy in the estimation of residual stresses and distortions using simplified CWM methods, achieving a required reliability level in manufacturing, and improving accuracy and reliability of local stress-based fatigue assessment methods.

Sammanfattning

I denna avhandling studeras de mekaniska egenskaper hos svetsade stålkonstruktioner, med focus på svetsdeformationer, svetsegenspänningar och utmattning. Noggrannheten i utvärdering av utmattningslivlängden, distorsion och.- svetsegenspänningsanalys med hjälp av Finitelement analys (Computational Weld Mechanics – CWM) studeras, samt inverkan av svetskvalitet, i form av geometrivariationer och spänningsgradient, på utmattningslivlängden.

Följande CWM-metoder har implementerats i de olika analyserna; termo-elastisk-plastiska, inneboende töjning (inherent strain), lokal och global modellering samt FE sub-strukturering både på T-kälsvetsförband och stumsvetsförband för att uppskatta svetsdeformationer och svetsegenspänningar.

För stora svetsade strukturer implementeras CWM-metoderna som använder lumping metoden, tillsammans med föreskriven temperaturlast, på svetsade lådkonstruktioner för att uppskatta svetsegenspänningarna. Analysen av svetsdeformationer har utförts på en stor svetsad balkkonstruktion experimentellt och numeriskt med hjälp av CWM-teknikerna, inherent strain, shrinkage och lumping. Metodernas noggrannhet studeras och förbättringar föreslås.

En probabilistisk modell utvecklas och implementeras för att uppskatta sannolikheten för förekomsten av ett önskat penetrationsdjup hos svetsförband samt för att uppskatta variationen. De ingående processparametrarna till den probabilistiska modellen är; spänning, ström, svetshastighet samt svetsens pistolvinkel studeras baserat på experimentella undersökningar. Svetsens inträngningsdjup utvärderas och mäts med hjälp av makrobilder tillsammans med ett digitalt verktyg utvecklats i Matlab. Den epistemistiska mätosäkerheten relaterad till utvärderingen kvantifieras och inkorporeras i den probabilistiska modellen.

Metoderna Hot Spot Spänning (HSS), 1-mm spänning (OM), Theory of Critical Distances (TCD), Stress Averaging (SA) och Effective Notch Stress (ENS) utvärderas för olika svetsförband och geometrier som utsätts för axiell-och böjbelastning med fokus på noggrannhet i predikteringen och tillförlitligheten hos de olika metoderna. Utvärderingen baseras på utmattningstestdata hämtade från litteraturen, samt utmattningsprovning utförd i denna studie. S/N-kurvor för utmattningsdimensionering föreslås för tex svetsade T-förband utsatta för böj-belastning för metoderna TCD och SA.

Monte Carlo-simulering implementeras för att beakta svetsgeometrins variationer i de lokala spänningsbaserade utmattningsbedömningsmetoderna (HSS-metoden, ENS-metoden, OM-metoden, TCD-metoden och SA-metoden). Den stokastiska variationen i svetsens tåradie, tåvinkel och a-mått baseras på de experimentella mätningarna. Noggrannheten hos de lokala spänningsbaserade utmattningsbedömningsmetoderna med

deterministisk och stokastisk SCF-fördelning (spänningskoncentrationer) bedöms mot experimentell data.

Publications

This doctoral thesis is based on the work presented in the following journal papers:

1. Zhu, J., Khurshid, M. & Barsoum, Z. Accuracy of computational welding mechanics methods for estimation of angular distortion and residual stresses. Weld World 63, 1391–1405 (2019). https://doi.org/10.1007/s40194-019-00746-9

J. Zhu planned the experimental work and measurements, carried out welding simulations, evaluated results and wrote the manuscript.

2. Zhu, J., Khurshid, M., & Barsoum, Z. (2019). Assessment of computational weld mechanics concepts for estimation of residual stresses in welded box structures. Procedia Structural Integrity, 17, 704-711. https://doi.org/10.1016/j.prostr.2019.08.094

J. Zhu planned the experimental work and measurements, carried out welding simulations, evaluated results and wrote the manuscript.

3. Zhu, J., Khurshid, M., Barsoum, I., & Barsoum, Z. (2021). Computational weld-mechanics assessment of welding distortions in a large beam structure. Engineering Structures, 236, 112055. https://doi.org/10.1016/j.engstruct.2021.112055

J. Zhu planned the experimental work and measurements, carried out welding simulations, evaluated results and wrote the manuscript.

4. Mansour, R., Zhu, J., Edgren, M., & Barsoum, Z. (2019). A probabilistic model of weld penetration depth based on process parameters. The International Journal of Advanced Manufacturing Technology, 105(1), 499-514.

https://doi.org/10.1007/s00170-019-04110-5

J. Zhu contributed in identifying the scientific gap, collecting the test results, writing some parts of the manuscript.

5. Zhu, J., Barsoum, Z., & Mansour, R. (2022). Numerical study of the influence of weld geometry variations on fatigue life using the notch stress analysis. Procedia Structural Integrity, 38, 621-630. https://doi.org/10.1016/j.prostr.2022.03.064

J. Zhu carried out finite element analysis, evaluated results and wrote the manuscript.

6. Zhu, J., Barsoum, I., Barsoum, Z., & Khurshid, M. (2022). Evaluation of local stress-based fatigue strength assessment methods for welded structures subjected to axial and bending loading. Fatigue & Fracture of Engineering Materials & Structures, https://doi.org/10.1111/ffe.13764

J. Zhu collected data from literature, carried out finite element analysis, evaluated results and wrote the manuscript.

Publications not included in the thesis

1. Zhu, J., Mansour, R. & Barsoum, Z. (2022). Analysis of the weld geometry variation using local stress-based fatigue assessment methods, manuscript ready to be submitted to International Journal of Fatigue.

2. Håkansson, J., Zhu, J., Barsoum, I & Khurshid, M. (2022). Fatigue strength assessment of cover plate joints subjected to axial and bending loading. manuscript ready to be submitted to Fatigue & Fracture of Engineering Materials & Structures.

Acronyms

CWM	Computational Weld Mechanics
ENS	Effective Notch Stress
SCF	Stress Concentration Factor
HSS	Hot Spot Stress
OM	1-mm Stress
TCD	Theory of Critical Distances
SA	Stress Averaging
MAG	Metal Active Gas
MIG	Metal Inert Gas
FE	Finite Element
FEA	Finite Element Analysis
ANN	Artificial Neural Network
IIW	International Institute of Welding
3D	3-Dimensional
RQ	Research Question
MC	Monte Carlo
PM	Point Method
LM	Line Method
AM	Area Method
VM	Volume Method
S-N	Applied stress against component life
FAT	Characteristic fatigue strength of the detail in MPa at 2 million cycles, and are assumed to represent a survival probability of 97.7%
MENS	Modified Effective Notch Stress
NS	Notch Stress

Chapter 1

Introduction

1.1 Background

Welding is the most common joining technique used to manufacture large structures such as cranes, wheel loaders, and trucks, etc. Metal active gas (MAG) together with metal inert gas (MIG) welding processes currently accounts for 70 to 80% of all manual and robot welding [1]. Owing to the shrinkage of melted metal, additional distortions and residual stresses are induced which have significant influence on structural functionality. To compensate for and correct the out of tolerance distortions, it is a common practice to use extra treatments such as flame straightening, mechanical pressing, and heat treatment [2,3]. The drawbacks of such treatments are extra labor hours, decreased production efficiency, inducing additional residual stresses due to these operations. Thus, it is of importance to minimize and control the welding distortion by optimizing the welding procedures.

Nowadays, digital tools involving Finite element (FE) simulations and databases possess of great potential to reduce the lead times of new developments by replacing the physical test loop [4]. One aspect of the digitalized welding process, as a tool for design and manufacturing, is to use CWM methods to estimate the mechanical response of welded structures. The thermo-elastic–plastic method is widely used to perform coupled and uncoupled thermo-mechanical Finite Element Analysis (FEA) with high accuracy predictions. However, the application of the thermo-elastic–plastic method on large welded structures is limited by the high level of computational time required. Thus, it is essential to develop and implement different numerical techniques for increasing the computational efficiency. The weld time cost versus simulation time cost of different welded structure using different CWM methods can be seen in *Table 1*. *Figure 1* shows a schematic illustration of the relation between accuracy, structural complexity and computational time for different CWM methods.

Table 1 Weld time cost versus simulation time cost

	Weld length (m)	Weld pass number (-)	Weld time cost (min)	Simulation time cost (min)
T-type fillet weld	0.26	1	0.55	Thermo-elastic-plastic: 510 Sub structuring: 480 Inherent strain: 240
Butt weld	0.1	2	1.95	Thermo-elastic-plastic: 1080 Sub structuring: 720 Inherent strain: 600
Box structure	1.6	40	66.67	Prescribed temperature: 1260
Beam structure	35.2	22	1260	Shrinkage method: 4800 Inherent strain: 1200

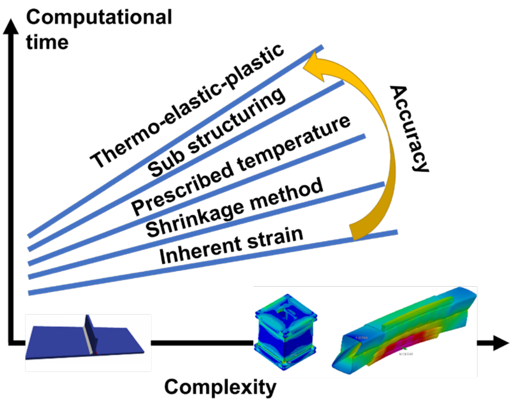

Figure 1 Schematic illustration of the relation between accuracy, structural complexity and computational time for different CWM methods

In welded structures, unwanted variation in weld geometry is typically observed. This is due to uncertainties in the process parameters which cannot be fully controlled. Physical trial and error tests are widely used in industry to ensure a desired weld geometry. Beside these, various predictive tools have been developed, such as mathematical models based on experimental results [5], artificial neural network (ANN) models [6], and numerical simulations [7]. However, the limitation of having uncertainties in those welding parameters is not addressed. Therefore, these studies cannot predict the influence of variation in welding parameters on the variation in the weld penetration depth. Establishing model for the probability of satisfying welding requirements is however crucial to ensure a required reliability level in manufacturing.

The fatigue strength assessment of welded structures is typically performed using stress-based, strain-based, and fracture mechanical based methods. The methods based on fracture mechanics include a specific analysis of crack growth which is not considered in the stress-based and strain-based methods. The strain-based methods could yield good estimation in the low and intermediate fatigue regime, due to the detailed analysis of local yielding [8]. The stress-based methods are usually applied to assess the fatigue strength in the high-cycle fatigue regime, where the number of cycles to failure exceeds 10^4 cycles [9]. For example, the nominal stress method, HSS method, and ENS methods are well-established methods in standards [10,11] and International Institute of Welding (IIW) recommendations [12]. Over the last few decades, various stress-based methods have been developed, which are simplified and computationally efficient, such as the OM method [13], TCD method [14], and SA method [15]. The schematic illustration of the relation between accuracy, complexity and effort for different fatigue strength assessment methods can be seen in *Figure 2*.

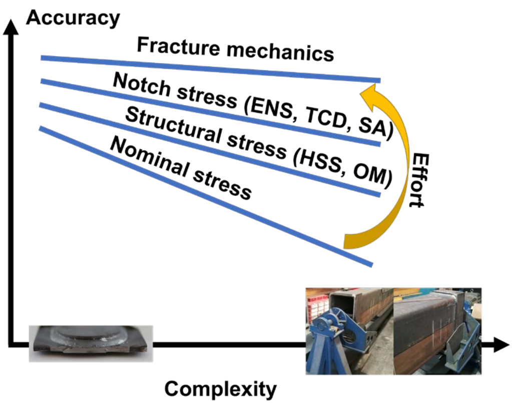

Figure 2 Schematic illustration of the relation between accuracy, complexity and effort for different fatigue strength assessment methods

The major limitation is that the variability in geometrical weld parameters is not included in the fatigue assessment. Instead, the FE analysis is based on only one idealized weld geometry and the fatigue strength is based on recommendations (which in their turn are developed based on fatigue testing). However, the local geometrical parameters generally vary stochastically along the weld. This is due to stochastic variabilities in the manufacturing process parameters that can hardly be eliminated. The geometrical parameters are found to have dominant contribution to the scatter in fatigue life. The disregard of the actual weld geometry effect can cause deviations between the estimated and real fatigue life [16]. It has been shown that these geometrical variations directly affect the scatter in fatigue life [17]. Detailed 3-dimensional (3D) FEA of welds have been performed to assess the influence of geometrical variability [18,19]. These methods are often based on the Weakest-link assumption [18,20]. However, performing such detailed analysis is generally computationally prohibitive, especially for practicing engineers. Using aforementioned stress-based methods which are simplified and computationally efficient with the local geometrical variations included could increase accuracy and reliability of fatigue strength assessments.

The validations of aforementioned stress-based methods for axial loading have been carried out in many studies, and an acceptable accuracy has been achieved. However, studies on applying the stress-based methods for welded structures subjected to bending are limited, especially for newly developed local stress-based methods. Baik et al. [21,22] found that bending obviously contributes to longer fatigue life than tension, because fatigue crack growth rate tends to be faster in the surface direction than in the depth direction. Since the fatigue strength is not often seen in fatigue design specifications for welded joints subjected to bending, using the fatigue strength under tension could estimate the fatigue life of welded joints under bending inaccurately [23]. Based on the reasons above, it is important to investigate the applicability, accuracy, and reliability of local stress-based methods for the fatigue strength assessment of welded joints under different loading conditions such as axial and bending loading.

1.2 Research questions and aim

The following aspects are found to be insufficiently addressed in the existing studies. The research questions (RQs) of the thesis are formulated thereafter.

- In regard to large welded structures, the accuracy of estimated distortions and residual stresses when using simplified approaches in numerical welding simulation are still doubtful and limitations in terms of quality in results need to be demonstrated. How to assess the welding distortions and residual stresses of large welded structures in good accuracy and efficiency? (RQ 1)
- The uncertainties in welding parameters are not considered. The influence of variation in welding parameters on the variation in the weld penetration depth is not addressed. How to ensure a required reliability level in manufacturing? (RQ 2)
- The variability in geometrical weld parameters is not included in the fatigue assessment. How would the weld geometry variations affect the fatigue strength assessments? (RQ 3) The applicability, accuracy, and reliability of local stress-based methods for the fatigue strength assessment of welded joints under bending loading is not well addressed. How to achieve good accuracy in the stress-based fatigue strength assessment of welded joints under bending loading? (RQ 4)

The aim of the research discussed within the current doctoral thesis is to develop methodology and concepts using CWM in order to increase the estimation accuracy in fatigue life assessment, distortion and residual stress analysis of welded structures:

- Assessing and improving the estimation accuracy of CWM methods for distortion and residual stress analysis. Propose cost-effective CMW approaches in order to boost the application of digitalization in welding industries and to reduce the number of trial-and-error tests.
- Establishing probabilistic models to predict the weld geometry, in the presence of weld process parameters uncertainties. Understand the effect of weld geometry variation on the scatter in fatigue life, in order to be incorporated in assessment methods increased fatigue life prediction accuracy.
- Incorporating geometry variations, welding deformation, axial and bending loading into fatigue strength assessment methods.

1.3 Research approach

Paper I: This study estimates the angular distortion and residual stresses due to welding using the following methodologies: thermo-elastic-plastic, inherent strain (local-global), and sub structuring on two types of welded joints (T-type fillet weld and butt weld).

Paper II: The finite element simulation using lumping method, together with prescribed temperature method, is implemented on welded box structures to estimate welding residual stress state.

Paper III: In this work, welding distortion analyses of a large welded beam structure are conducted experimentally and with the CWM techniques: inherent strain (local–global) method and shrinkage method combined with the lumping approach.

Paper IV: In this work, a probabilistic model is proposed to estimate the probability of satisfying a desired penetration depth as well as to predict its variation. The uncertain process parameters are voltage, current, travel speed, and torch travel angle which were studied based on an experimental investigation.

Paper V: In this work, we use Monte Carlo (MC) simulation to study the influence of these stochastic variations on the probability distribution of fatigue life. A non-load carrying fillet cruciform joint is studied based on notch stress approaches.

Paper VI: In the study, the local stress-based fatigue strength assessment methods are used: the HSS method, OM method, TCD method, SA method, and ENS method, to assess their accuracy and reliability for welded joints subjected to axial and bending loading. Fatigue design curves applicable for T-joints under bending are proposed, which can be used in conjunction with the TCD method and SA method.

Welding process	Weld quality	Distortion and residual stress	Fatigue		Experiment	Simulation
Input		RQ 1		Paper I	T-joints & Butt joints	CWM
Input		RQ 1		Paper II	Box structure	CWM
Input		RQ 1		Paper III	Beam structure	CWM
Input	RQ 2			Paper IV	Fillet weld	Probability model
	Input		RQ 3	Paper V		FE
		Input	RQ 4	Paper VI	T-joints & cover plate	FE

Figure 3 Illustration of the link between the appended papers and RQs

The connection of the appended papers and RQs is presented in *Figure 3*. In this thesis, an overview of CWM methods for distortions and residual analysis and fatigue strength assessment methods is presented in Chapter 2. For distortion analysis, Thermo-elastic-plastic method, Inherent strain (local-global) method, Sub structuring method, Shrinkage method are discussed in Chapter 2.1. The CWM methods (Lumping method, Prescribed temperature method) are presented in Chapter 2.2. The fatigue strength assessment methods are shown in Chapter 2.3. In Chapter 3, the appended papers is summarized. Conclusions are made to address the research questions in Chapter 4. Contribution to research field and the future work can be seen in Chapter 5 and 6.

Chapter 2

Computational weld mechanics

2.1 Distortions

The welding deformations caused by the shrinkage of filler material can be divided into several types. Transverse shrinkage and angular distortion are caused by shrinkage perpendicular to the weld bead. For a long butt weld, rotational distortion led by this transverse shrinkage may occur. Longitudinal shrinkage, longitudinal distortion, and buckling are due to shrinkage along the weld bead. *Figure 4* illustrates the basic classification of deformation induced by welding.

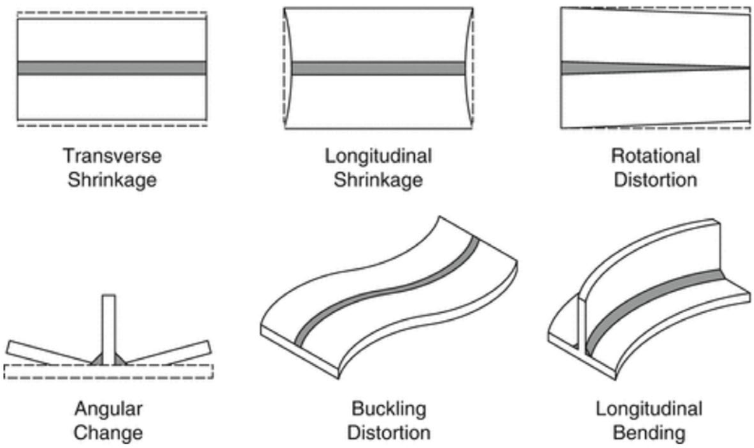

Figure 4 Classification of welding distortion [24]

2.1.1 Thermo-elastic-plastic method

The thermo-elastic–plastic method is widely used to perform coupled [2,25] and uncoupled [26,27] Thermo-mechanical FEA on small scale specimens such as T-type fillet and butt welds, because of its high accuracy. Its application to large welded structures is rarely seen, due to the high computational time required, complexity and the amount of welding associate with large welded structures.

2.1.2 Inherent strain (local-global)

The concept of inherent strain was developed by Ueda et al. [28]which can be expressed in its simple form as

$$\varepsilon^* = \varepsilon - \varepsilon^e \tag{1}$$

The constitutive relation for an elastic material using inherent strain concept following Hooke's law is given by [29]

$$\{\sigma\} = [C](\{\varepsilon\} - \{\varepsilon^*\}) \tag{2}$$

Where σ denotes the stress, C denotes the elastic constitutive matrix, ε denotes the total strain, ε^e denotes the elastic strain and ε^* denotes the inherent strain.

When the structure cools down to room temperature and unclamping takes place, it is assumed that thermal strain vanishes and the inherent strain ε^* as assumed to equal the plastic strain ε^p [30,31], where strain due to phase transformation and creep are neglected.

The inherent strain (local-global) method needs plastic strains calculated from a local 3D model with thermo-elastic-plastic method as input, see *Figure 5*. Afterwards, the elastic FE analysis of the global model is carried out.

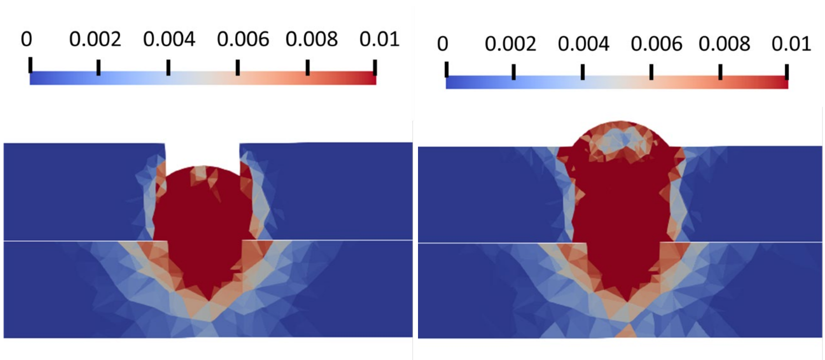

(a) (b)

Figure 5 Inherent strain distribution, (a) after the first weld pass and (b) after the second weld pass[32].

Thus, the definition of the local model is very important. The influence of the local boundary condition has been highlighted by Souloumiac [31]. The boundary condition of the local model should be close to reality [33]. Duan et al. [34] developed a well-defined method of determining the size and boundary condition of local models. They concluded the local model size should be able to retain the same temperature history as the global model. The concept of "rigid border" boundary condition was defined by using a rigid part added to the frontier of the local model to keep the boundary in plane. In order to represent the mechanical conditions imposed by the rest of the structure, the rigidity of the rigid part may be changed by adjusting the value of Young's modulus. In this study, the local model size and local boundary condition are defined according to Duan's work [34].

As shown in *Figure 6*, the level of accuracy is increased with the decrease of the block period and the curve trends for the T-type fillet weld and butt weld are similar. In addition, erroneous results could be observed when very short block period is applied as the plastic strain is extracted when the structure cools down to room temperature. It is suggested that an appropriate block period be considered in the inherent strain (local-global) method.

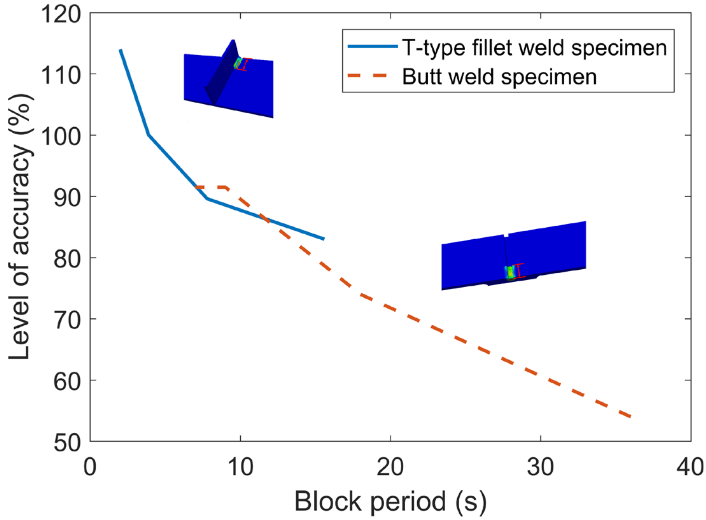

Figure 6 Influence of block period on accuracy in the inherent strain method [35].

2.1.3 Sub structuring

The simulation model using the sub structuring technique is performed by dividing the entire structure into two parts: the linear region and the nonlinear region, see *Figure 7*. The elastic isotropic material model is assigned to the linear region with almost elastic behaviour during the welding process. The elastic-plastic material model, assuming isotropic hardening, is applied to the nonlinear region which is close to the heat source.

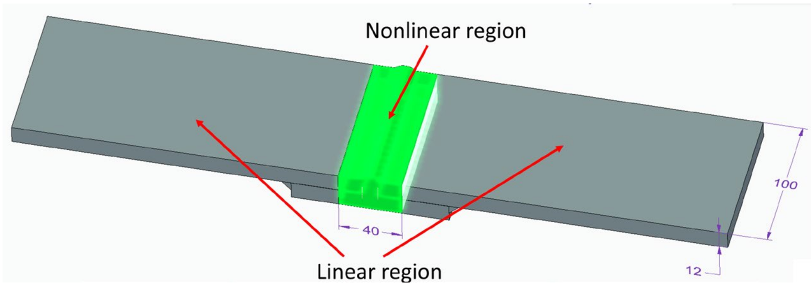

Figure 7 Linear and nonlinear regions in the sub structuring method[35].

2.1.4 Shrinkage method

The shrinkage approach is based on a linear elastic FEA where the linear thermal contraction of the weld metal is assumed to be the main driving force for welding distortion [36]. In the shrinkage approach, the elements within the shrinkage zone are initially assigned a melting temperature, which is changed to room temperature at the end of the computational step. The contraction is resisted by the surrounding parent metal, resulting in the formation of internal forces [36]. The relation between the forces and deformation in the linear elastic FEA is given by the following equations [37]:

$$\{x\} = [k]^{-1}\{F\} \tag{3}$$

$$\{\theta\} = [k_0]^{-1}\{M\} \tag{4}$$

where x, θ, k, k_0, F and M denote the shrinkage deformation (mm), angular distortion (rad), equivalent shrinkage stiffness of the weld-affected zone (N/mm), equivalent bending stiffness of weld-affected zone (Nmm), equivalent shrinkage force (N) and equivalent bending moment (Nmm).

The shrinkage zone size can be determined by the plastic zone size obtained from the thermo-elastic-plastic analysis [38,39], see *Figure 8*. Compared to the inherent strain (local-global) approach, the material properties applied in the shrinkage approach can be assumed as constant, which significantly reduces the efforts in welding simulations. The yield strength and Young's modulus were found to be the most important material parameters for the estimation of distortions in the shrinkage approach [38].

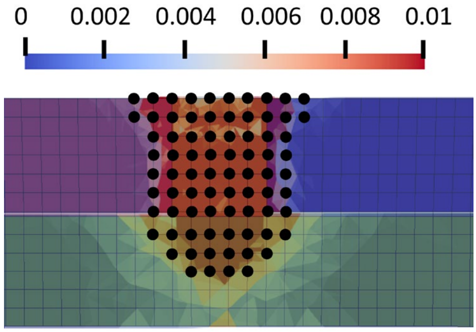

Figure 8 Shrinkage zone size[32].

2.2 Residual stresses

The welding residual stresses result from the restraints of adjacent base metal during the shrinkage of melted metal. The stresses perpendicular to the weld line are defined as transverse residual stresses and the stresses parallel to the weld line are defined as longitudinal residual stress. The magnitude of residual stresses in and near to the weld can be up to material yield strength magnitude in highly constrained cases, which has a very significant effect on fatigue [40]. The welding residual stresses distribution can be influenced by the structural factors (geometry [41], type of weld joint, fixtures [42]), welding process parameters (welding sequence [43], heat input [44]) and properties of base and filler materials [41].

2.2.1 Lumping method

In the lumping approach, several welding passes are lumped into a large pass [45,46]. The lumping approach has been used for the welding process having multi-passes to reduce simulation time [46,47]. Hu et al. [48] found that lumping weld passes along the thickness direction has little effect on the accuracy of the residual stresses, while lumping weld passes along the width direction could cause an underestimation of the transverse residual stresses. The longitudinal residual stresses in both cases can be estimated with a reasonable accuracy. Malmelöv et al. [49] concluded that the accuracy for the resulting temperatures and deformations can be retained with a considerable reduction in computation time.

In Paper II, the five weld passes were lumped into two weld passes, which reduces the total number of weld passes from 40 to 16. The first three weld passes were lumped into one pass defined as lump-pass 1 and the last two passes were lumped into another pass defined as lump-pass 2, as shown in *Figure 9*. The total heat input of lump-pass weld Q is shown in Eq.(5).

$$Q = \eta \sum_{1}^{n} U_n I_n \tag{5}$$

Where η is welding efficiency, U is voltage, I is current, n is weld pass. The welding efficiency η and the welding speed of lump-pass were calibrated based on the temperature measurements. The moving welding arc was modeled as the double ellipsoid distribution developed by Goldak [50]. The parameters of double ellipsoid model were calibrated according to the match between the macrographs and the isothermal contour plots for the fusion zone. The results from the thermal analysis for the two lump-pass welds are presented in *Figure 10*.

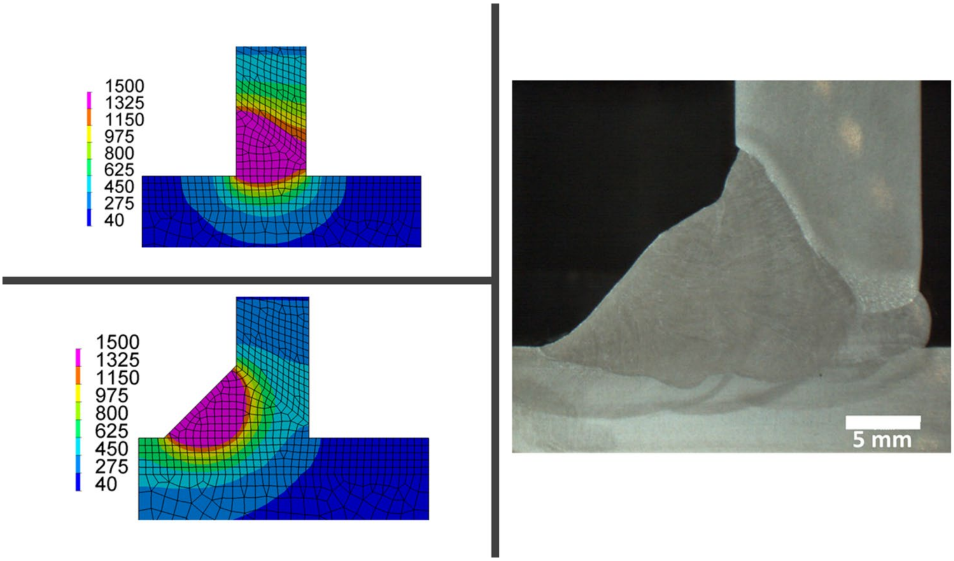

Figure 9 Lumped passes and macrograph [47].

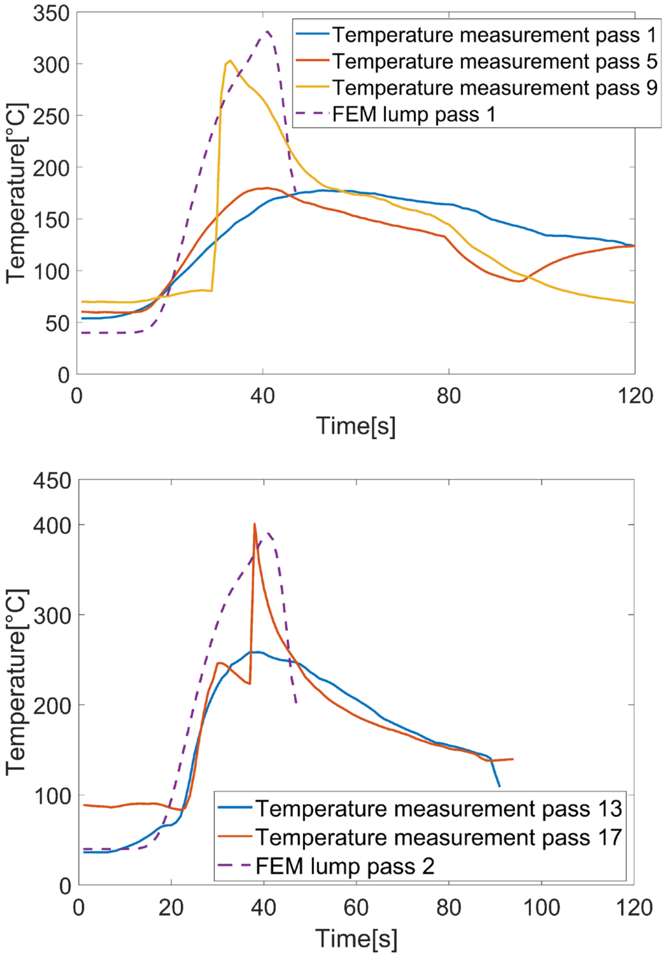

Figure 10 Experimental and numerical temperature history of weld passes [47].

2.2.2 Prescribed temperature method

In the prescribed temperature method, the prescribed temperature curve was calculated from Thermal-elastic-plastic method using a moving heat source. The temperature history of the nodes in the molten zone was averaged. Afterwards, the averaged temperature history curve was applied on the entire weld bead assuming the infinite welding speed in the sequential thermomechanical welding simulation. Lindgren et al. [51] used the prescribed temperature method as a means for heat input to study the residual stress state as a result of multi pass butt welding of a very thick plate.

In Paper II, the temperature curves of all the nodes in the molten zone with temperatures equal or above 1500°C were averaged and made into the prescribed temperature curve which is shown in *Figure 11*a. The prescribed temperature curve was applied on all the nodes associated with a weld, see *Figure 11*b. This corresponds to the weld with infinite welding speed.

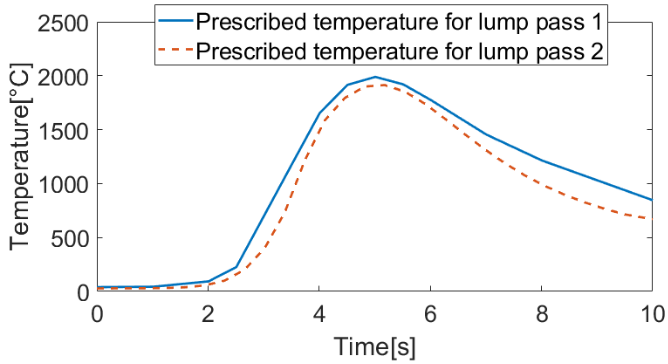

(a)

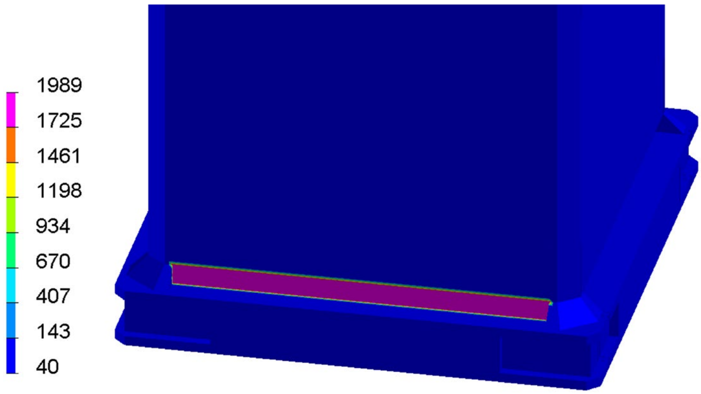

(b)

Figure 11 (a) Prescribed temperature for lump pass 1 and 2; (b) Temperature distributions[47].

2.3 Welding, weld quality and Fatigue

2.3.1 Weld geometry uncertainties

2.3.1.1 Welding parameters and sources of uncertainty

The travel speed is the linear rate with which the torch arc moves along the weld bead. A schematic illustration of the torch arc movement is shown in *Figure 12*a. Conservatively, the travel speed may vary by ±10% of the pre-set value due to undesirable vibration or backlash.

The torch travel angles, defined in *Figure 12*a, is set using a digital angle gauge. Various factors result in variation in the torch travel angle, such as limited repeatability in robots and inaccuracies of measuring devices. The assumption is that the uncertainty is ±3 degrees of the setting value. It should be observed that this variation is assumed to be the same regardless of the pre-set value.

The voltage is pre-set at the power source which has a constant voltage characteristic. However, the dynamic characteristic of the welding arc, under the influence of electric and thermal conductivity of arc and arc length [52], results in variations in both voltage and current. The power source makes simultaneous millisecond changes in both voltage and current, in order to maintain a stable arc condition. Thus, during welding, the voltage and current are correlated [53]. The typical volt-ampere characteristic for constant voltage power source can be seen in *Figure 12*b. The slope α defined as

$$\alpha = -\frac{\Delta V}{\Delta I} \tag{6}$$

is used to compute the statistical correlation between voltage and current. A value of α being 0.02 V/A is used for robotic MAG welding, which was verified both mathematically and experimentally [53].

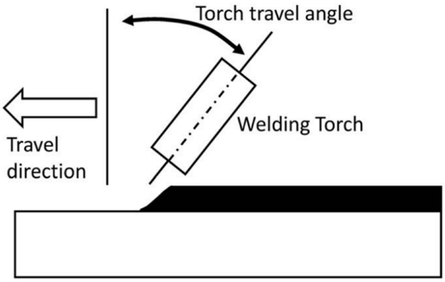

(a)

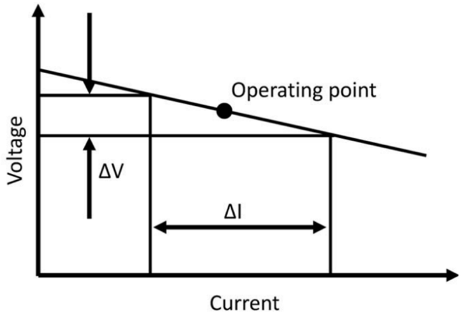

(b)

Figure 12 Illustration of welding parameters: (a) Travel direction and torch travel angle. (b) Volt-ampere characteristic for constant voltage power source [54].

2.3.1.2 Variations in weld geometry

The measurements of local geometrical parameters such as toe angle, toe radius and throat thickness shown in *Figure 13*a are described in [17]. In the manual welding, the data points number is 40, and the mean values of the toe angle, toe radius and throat thickness are 49°, 0.95 mm and 6 mm. The corresponding standard deviations are 7.5°, 0.9 mm and 0.3 mm. In the robotic welding, the data points number is 23, and the mean values of the toe angle, toe radius and throat thickness are 49°, 1.4 mm and 5.4 mm. The corresponding standard deviations are 9.8°, 0.8 mm and 0.2 mm. Since the geometry values in manual welding and robotic welding are similar, the two groups of data are combined. The combined mean values of the toe angle, toe radius and throat thickness and the corresponding standard deviations are calculated using Cochrane's formula [55], which are 49°, 8.33°, 1.11 mm, 0.89 mm, 5.78 mm, and 0.39 mm. The toe angle, toe radius and throat thickness are described as lognormal distribution because of the positive sign of the three geometry parameters, see *Figure 13*b.

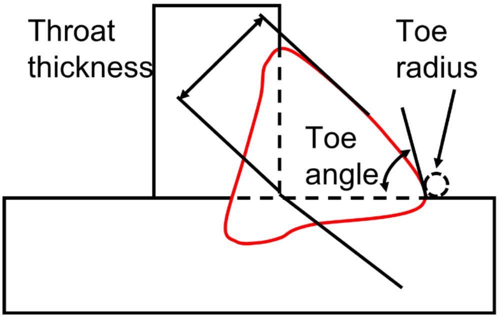

(a)

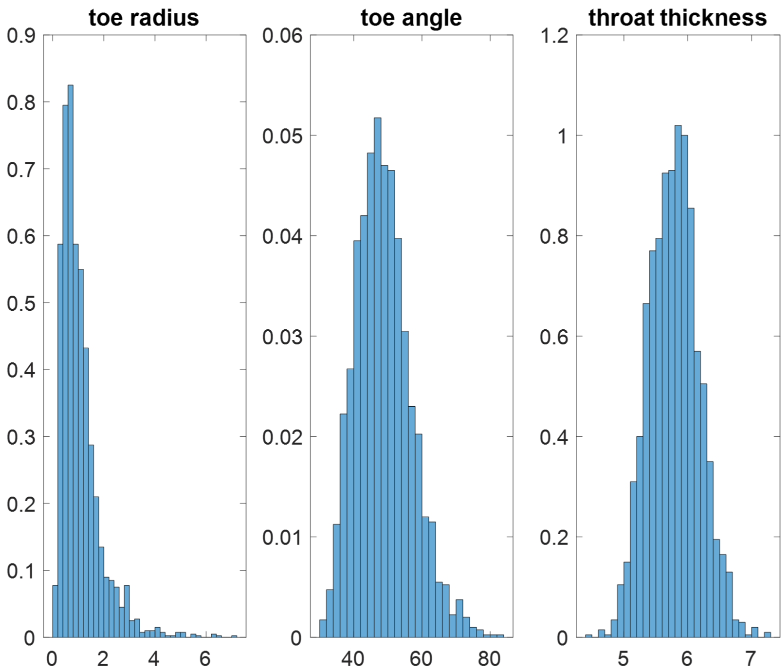

(b)

Figure 13 (a) Geometry parameters, (b) Lognormal distribution of geometry parameters.

2.3.2 Fatigue strength assessment methods

2.3.2.1 Hot spot stress (HSS) method

The HSS method is one of several ways to describe the structural stress originally developed within the offshore industry. The structural stress is also referred to as geometric stress, which considers the effects of a structural discontinuity and is characterized by membrane and shell bending stress. The HSS method is only applicable to weld toe failures and not weld root failures. There are two types of HSS, which are distinguished according to the location on the plate and orientation to the weld toe. Type *a* HSS is transverse to weld toe on the plate surface, and type *b* HSS is transverse to weld toe at plate edge [12]. The HSS can be determined using the linear/quadratic extrapolation of surface stresses [12], (see *Figure 14*a) or the stresses through thickness direction [56]. In this study, the linear extrapolation of surface stress is applied to calculate the hot spot stress σ_{hs}, see Eq.(7).

$$\sigma_{hs} = 1.67\sigma_{0.4t} - 0.67\sigma_{t} \tag{7}$$

where $\sigma_{0.4t}$ and σ_{t} are the stresses parallel to the loading direction at a distance of $0.4t$ and t from the weld toe, and t is the plate thickness. The quadratic extrapolation is suitable for the case where the stress gradient is steeper [56]. In the HSS method, the FAT class, e.g. the characteristic fatigue strength of the detail in MPa at 2 million cycles, depends on the structural details and loading conditions.

2.3.2 1-mm stress (OM) method

The OM concept has been proposed by Xiao and Yamada [23], which is another way of assessing structural stress from a fatigue perspective. The non-linear stress peaks due to the local weld profile are excluded, especially the notch effect of the weld toe transition. Compared to the HSS method, the OM method can account for the size and thickness effect, which results in a reduction of fatigue strength with increasing plate thickness. Because the stress gradient through thickness is considered in the OM method [23]. The stress parallel to the loading direction at 1 mm below the weld toe or the location of expected crack is defined as the 1-mm stress σ_{s}, see *Figure 14*b. Xiao et al [13][23] proposed different FAT classes for axial loading and bending. FAT 100 is suggested for welded joints under axial loading with a positive stress ratio. FAT 125 is recommended for welded joints under bending with $R = 0.1$. *m* is set to be 3 for axial loading and bending [13][23].

2.3.3 Theory of Critical Distances (TCD) method

The TCD methods introduced by Taylor [57] are the Point Method (PM), Line Method (LM), Area Method (AM), and Volume Method (VM). The effective stress in the PM is defined as the stress at a fictitious point (*Figure 14*c). The effective stress in the LM, AM, and VM is defined as the average stress over a line, area, and volume. In the current study, the PM is used because the accuracy of the PM and LM are similar, and more accurate results are hardly achieved using more complicated AM and VM [57]. The effective stress in the PM can be expressed using Eq. (8) [57,58].

$$\sigma_{eff} = \sigma(\theta = 0, r = a) \tag{8}$$

where a is the critical distance which can be determined through the theoretical equation $\rho^* = 4a$ and ρ^* is a microstructural support length [58]. An appropriate choice of ρ^* for steel can be derived based on experimental investigations and Neuber's micro-support theory, resulting in $\rho^* = 4a$ mm and $a = 0.1$ mm [58–60]. Baumgartner et al. [58] found that $a = 0.1$ mm also resulted in the lowest scatter in the S-N curves, and FAT 160 was recommended when using the maximum principal stress.

2.3.4 Stress averaging (SA) method

The SA method is one of the elastic notch stress methods, which considers the local notch radius, the microstructural support effect of the material, and stress gradient in the local notch. The method is initially proposed by Neuber [15]. In the SA method, the effective stress is the stress averaged over a length ρ^* from the notch tip[15,58,59], see Eq.(9) and *Figure 14*d.

$$\sigma_{eff} = \frac{1}{\rho^*}\int_0^{\rho^*} \sigma(r)dr \tag{9}$$

The relationship between the maximum stress and the effective stress can be expressed as Eq. (10), where η is notch sensitivity factor and n is support factor.

$$\frac{1}{\eta} = n = \frac{\sigma_{\max}}{\sigma_{eff}} \tag{10}$$

In the SA method, the notch radius could be an actual notch radius, an average radius, or a minimal notch radius assumed to represent the worst case [61]. When using maximum principal stress, a microstructural length $\rho^* = 0.4$ mm and FAT 160 are recommended [58].

2.3.5 Effective notch stress (ENS) method

Radaj [62] introduced the fictitious radius to replace sharp notches in the ENS method, based on Neuber's theory. This fictitious notch radius ρ_f can be written as $\rho_f = \rho + s\rho^*$, where ρ is the actual sharp notch radius, s is a multiaxiality factor. For plane strain condition at the sharp notch, the multiaxiality factor is set to $s = 2.5$, yielding

$s\rho^{*} = 1$ mm. A worst-case scenario is achieved by setting the actual notch radius to $\rho = 0$ mm, resulting in an effective notch radius of $\rho_f = 1$ mm [59]. For thin-walled structures where the plate thickness is less than 5 mm, the fictitious notch radius $\rho_f = 0.05$ mm might be applied to avoid the weakening of cross sections of plates [63]. The effective notch stress is obtained as the maximum stress at the fictitious notch radius, which is calculated from the finite element analysis (FEA), see *Figure 14*e. The design curve with FAT 225 and $m = 3$ is recommended for the ENS with $\rho_f = 1$ mm [12].

2.3.6 Modified Effective Notch Stress (MENS) method

In the MENS method, the actual weld dimensions such as actual weld toe radius, weld toe angle and weld throat thickness can be considered. The fictitious notch radius depends on the weld geometry, instead of using the fictitious notch radius $\rho_f = 1$ mm. Schijve [64] recommended the fictitious notch radius can be determined using $\rho_f = 0.1t$. For the MENS method in this study (*Figure 14*f), the fictitious notch radius can be defined in Eq.(11) [65]

$$\rho_f = \rho_{actual} + 1 \tag{11}$$

where ρ_{actual} is the actual radius of the weld toe. A lower design S-N curve is proposed with FAT 200, compared to FAT 225 for the fictitious notch radius $\rho_f = 1$ mm [65,66]. The design S-N curve is valid for relatively sharp weld toe radius less than 3 mm, and a minimum notch factor 1.6 is recommended, which is the ratio of the effective notch stress to the structural stress.

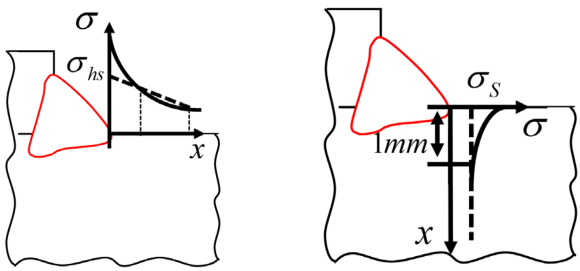

(a) (b)

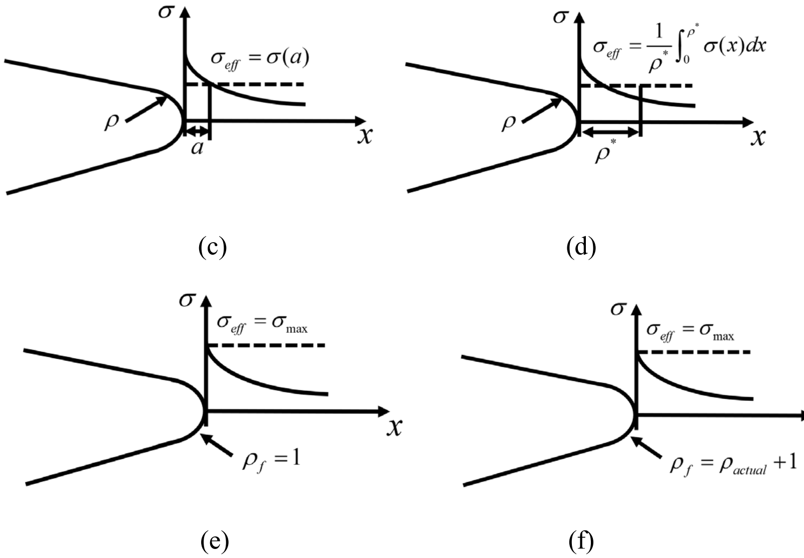

Figure 14 Illustration of (a) HSS method, (b) OM method, (c) TCD method, (d) SA method, (e) ENS method, (f) MENS method.

Chapter 3

Summary of the appended papers

3.1 Paper I

The welding deformations and residual stresses in a structure may influence the functionality, safety, and durability. Thus, it is of significant importance to reduce adverse deformation and residual stresses. Traditionally, trial and error tests are used to solve these problems. Their drawbacks are that they are time-consuming and expensive. Nowadays, digital tools involving FE simulations and databases possess of great potential to reduce the lead times of new developments by replacing the physical test loop. Due to the high level of computational time necessary in the thermo-elastic-plastic method, the applications of simplified CWM approaches are needed and their accuracy should be studied.

In this study, the following FE simulation methods: thermo-elastic-plastic, inherent strain (local-global), and sub structuring have been implemented both on T-type fillet weld and butt weld specimens to estimate angular distortion and residual stresses. The numerical results are compared with the experimental measurements and these methodologies are evaluated in terms of accuracy and computational time. In addition, the influence of welding sequence on distortion and transverse residual stresses has been studied numerically by implementing the thermo-elastic-plastic and inherent strain (local-global) methods on the T-type fillet weld.

3.2 Paper II

The residual stresses have a vital effect on the fracture and fatigue behaviors of the welded structures. Thus, it is of significant importance to quantify welding residual stresses from a structural integrity point of view. The Thermo-elastic-plastic method has been widely applied to different types of small welded structures because of its high accuracy. However, the application of the Thermo-elastic-plastic method on large welded structures is limited by the high level of computational time required. Thus, it is essential to develop and implement different numerical techniques for increasing the computational efficiency.

In this study, the finite element simulation using lumping method, together with prescribed temperature method, is implemented on welded box structures to estimate welding residual stress state. The simulations have been performed using commercial software: SYSWELD. The thermal history from simulations has been verified with experimental measurements. Residual stress measurements at the weld toe side were carried out by X-ray diffraction technique. Moreover, a sub model of the welded box type structure is studied using the following computational weld mechanics concepts: Thermo-elastic-plastic, lumping and prescribed temperature, in order to assess the computational time and the magnitude of estimated residual stresses of those concepts.

3.3 Paper III

Unwanted distortions are typically observed in components after the welding process. Physical trial tests and extra post-treatments are being widely utilized in industries to minimize and correct the out of tolerance distortions. These methods are time-consuming and costly. There has been growing interest in digital tools which have great potential to minimize the physical test loops and corrections. Although a number of CWM methods are available today, the validation of most simplified simulation methods in the literature are not sufficient. In regard to large welded structures, the accuracy of estimated distortions and residual stresses when using simplified approaches in numerical welding simulation are still doubtful and the limitations in terms of quality in results need to be demonstrated.

In this study welding distortions analysis has been carried out on a large beam structure experimentally and numerically using CWM techniques such as the inherent strain (local–global) method and the shrinkage method, together with the lumping approach. Temperature history, distortions, and residual stresses were measured experimentally. The numerical results are compared with experimental measurements to quantify the accuracy.

3.4 Paper IV

In welded structures using robotized MAG welding, unwanted variation in penetration depth is typically observed. Weld penetration depth is one of the critical weld profile parameters that have significant influence on fatigue life and structural integrity. Therefore, physical trial and error tests are widely used in industry to ensure a desired weld penetration depth. Beside these, various predictive tools have been developed, such as mathematical models based on experimental results, ANN models, and numerical simulations. However, the limitation of having uncertainties in those welding parameters is not addressed. Therefore, these studies cannot predict the influence of variation in welding parameters on the variation in the weld penetration depth. Moreover, to the best of the authors' knowledge, there is no established model for the probability of satisfying welding requirements, in terms of weld penetration depth. Predicting this probability is however crucial to ensure a required reliability level in manufacturing.

In this work, a probabilistic model is proposed to estimate the probability of satisfying a desired penetration depth as well as to predict its variation. The uncertain process parameters are voltage, current, travel speed, and torch travel angle which were studied based on an experimental investigation. The weld penetration depth is evaluated from macrographs using a digital tool developed in MatLab. The epistemic measurement uncertainty related to this evaluation is quantified and incorporated in the probabilistic model.

3.5 Paper V

A wide range of engineering structures rely on welded joints for proper structural integrity. These joints are often the limiting factor for the fatigue strength of such structures. A widely used simplified and computationally efficient fatigue assessment method is based on the notch stress (NS) method. The notch stress is computed by FEA with a certain assumed notch radius and an idealized geometry [12]. The stress range is obtained as the product of the applied nominal stress range and the SCF due to the local notch. Studies demonstrate that the choice of the idealized weld geometry in the notch stress analysis is still not clear, especially when the geometrical variations are large [67][68]. The variability in geometrical weld parameters is not included in the fatigue assessment. Instead, the notch stress analysis is based on only one idealized geometry and a FAT-value based on recommendation. However, the local geometrical parameters generally vary stochastically along the weld, which is found to have a non-trivial influence on fatigue life.

To address this limitation, it is essential to include the local geometrical variations when assessing the fatigue life. In this work, we use MC simulation to study the influence of these stochastic variations on the probability distribution of fatigue life. A non-load carrying fillet cruciform joint is studied based on two notch stress approaches with different reference toe radius and FAT values: $\rho_f = 1$ mm with FAT 225 and $\rho_f = \rho_{actual} + 1$ mm with FAT 200. Both approaches are compared with respect to their fatigue life prediction as well as the predicted influence of geometry variability.

3.6 Paper VI

The stress-based methods are usually applied to assess the fatigue strength in the high-cycle fatigue regime. The nominal stress method, HSS method, and ENS methods are well-established methods in standards, and IIW recommendations. Over the last few decades, various stress-based methods have been developed, such as the OM method, TCD method, and SA method. The validations of the HSS method, ENS method, OM method, TCD method, and SA method for axial loading have been carried out in many studies, and an acceptable accuracy has been achieved. Studies on applying the stress-based methods for welded structures subjected to bending are limited, especially for newly developed local stress-based methods. Since the fatigue strength is not often seen in fatigue design specifications for welded joints subjected to bending, using the fatigue strength under tension could estimate the fatigue life of welded joints under bending inaccurately.

The HSS, OM, TCD, SA, and ENS methods are evaluated in terms of accuracy and reliability. The evaluation is based on fatigue test data extracted from the literature and carried out in this study.

Chapter 4

Conclusions

The studies presented in this thesis aim to develop methodology and concepts using CWM in order to increase the estimation accuracy in fatigue life assessment, distortion and residual stress analysis of welded structures.

To address RQ 1, Paper I-III conducted welding distortions and residual stresses analyses of small-scale specimens and large welded structures experimentally and with the CWM techniques.

- The estimated angular distortion and residual stresses in front of the weld toe from the thermo-elastic-plastic, inherent strain (local-global), and sub structuring methods are in good agreement with the experimental measurements of T-type fillet welds.
- Sub structuring method can reduce computational hours by up to 30% as compared to the thermo-elastic-plastic method. The inherent strain (local-global) method is very time-efficient compared with the others, but it needs plastic strains as input.
- For the inherent strain (local-global) method, the influence of block length on estimated angular distortion is significant. Reducing the block length results in an increased angular distortion and reduced level of underestimation.
- The prescribed temperature method can reduce the computational time by 80% as compared to the Thermo-elastic-plastic method. Furthermore, the computational time for using lumping method, together with prescribed temperature method is 65% less than the prescribed temperature method. However, the magnitude of residual stresses may be underestimated.
- The shrinkage zone size has a significant influence on the accuracy of estimated distortions using the shrinkage approach. The accuracy of estimated distortions increases when the shrinkage zone is set to be close to the plastic strain zone size calculated from the thermoelastic–plastic method.
- For the butt weld specimen and beam structure, the estimated distortions from the shrinkage together with lumping approaches are in good agreement with the experimental measurements and the computational time is affordable.
- The trends of estimated distortions using inherent strain (local–global) match with the experimental measurements. However, the magnitude of distortions could be underestimated if the computational steps of activating the plastic strain in the welds are not enough.

A probabilistic model is proposed in Paper IV to estimate the probability of satisfying a desired penetration depth as well as to predict its variation, which will contribute to bridge the research gap discussed in RQ 2.

- When a reliability level of 90% is required, the proposed probabilistic model yields process parameters set-ups that differs significantly compared with a traditional deterministic approach. This is due to the fact that deterministic approaches yield reliability levels close to 50% regardless of the input uncertainties.
- Using the proposed probabilistic model, it is concluded that the uncertainty in welding current shows the largest contribution to the variation in the weld penetration depth. Therefore, in order to limit this variation, the capability of power sources to control and provide required characteristics has to be enhanced.

In Paper V, MC simulation is applied to study the influence of these stochastic variations on the probability distribution of fatigue life in RQ 3. In Paper VI, the HSS, OM, TCD, SA, and ENS methods are evaluated in terms of accuracy and reliability for welded structures (cover plates and T-joints) subjected to axial and bending loading (RQ 4). The evaluation is based on fatigue test data extracted from the literature and carried out in this study.

- The stochastic NS method with $\rho_f = 1$ mm and FAT 225 yields roughly the same predicted fatigue life as when deterministic (mean) values for the leg length and toe angle are used.
- The Stochastic NS method with $\rho_f = \rho_{actual} + 1$ mm and FAT 200, predicts a lower fatigue life compared to using deterministic (mean) values of leg length, toe angle and toe radius.
- Large misalignments affect the stress considerably and need to be considered in the fatigue strength assessment of cover plate joints under axial loading.
- SA method can be used to assess the fatigue strength of cover plate joints under axial loading with relatively good accuracy and low scatter, followed by the ENS method.
- The OM method is not applicable to T-joints with small plate thickness ($t \leq 6$ mm) subjected to bending.
- The fatigue strength assessment of T-joints subjected to bending using the current fatigue design curves in the HSS method, TCD method, SA method, and ENS method is excessively conservative, and the accuracy and reliability are low.
- Higher accuracy and lower scatter in the TCD method and SA method could be achieved using fatigue design curves $m = 5$ with FAT 298 and 263 for T-joints with plate thickness $t \leq 7$ mm subjected to bending.

Chapter 5

Contribution to research field

- The accuracy of the CWM methods (thermo-elastic-plastic, inherent strain (local-global), and sub-structuring) on the estimation of distortions and residual stress of small-scale specimens has been studied and improvements have been proposed for inherent strain (local-global) method.
- The evaluation of simplified CWM methods (lumping method, prescribed temperature method, inherent strain (local–global) method and shrinkage method) are based on large-welded structures in terms of the accuracy of estimated distortions and residual stresses.
- The effects of various welding process parameters (i.e. welding sequence, fixture, and weld pool size) on welding distortions were investigated.
- A probabilistic model is proposed to estimate the probability of satisfying a desired penetration depth as well as to predict its variation. The model is crucial to ensure a required reliability level in manufacturing.
- The influence of weld geometry variations is assessed in the ENS fatigue assessment methods.
- The HSS method, ENS method, OM method, TCD method and SA method are evaluated under the axial loading and bending in terms of accuracy and reliability.
- Fatigue design curves applicable for T-joints under bending are proposed, which can be used in the TCD method and SA method.

Chapter 6

Future work

Paper I to III focus on assessing and improving the estimation accuracy of CWM methods for distortion and residual stress analysis. The experimental measurements are critical to the work. The measuring approach for distortions and residual stresses can be improved, such as using laser measuring instruments for measuring distortions and using smaller collimator in X-ray diffraction for residual stresses measurements. Furthermore, the residual stresses status through the thickness of the plate could also be good inputs for assessing the accuracy of CWM methods. Modelling technique in CWM methods can be improved to increase the accuracy and efficiency, especially for the inherent strain (local-global) method. Because it is found that activating the plastic strain with an appropriate number of blocks can improve the accuracy of estimated angular distortion. According to the weld length and weld speed, the number of blocks is approximately 200 for each weld pass. However, the computational time required will rise considerably for the current model using solid elements. Hence, a model using shell elements is recommended in further studies.

Paper IV proposed a probability model which can be used to estimate process parameters set-ups that satisfy a desired reliability level. In the future, the model can be further developed to establish a link between the process parameters set-ups and the performance of welded structures. Furthermore, the work paves the way for data-driven manufacturing which implies that decisions controlling the manufacturing process are based on analysis of collected data. The challenge would be large amounts of data is needed during the manufacturing process, testing and measurements.

Reference

[1] Claes O (2017) Design handbook for welded steel products. ISBN 9789198152913. p 53.

[2] Mondal AK, Biswas P, Bag S. Prediction of welding sequence induced thermal history and residual stresses and their effect on welding distortion. Weld World 2017;61:711–21. https://doi.org/10.1007/s40194-017-0468-3.

[3] Michaleris Pan. Minimization of welding distortion and buckling: modelling and implementation. Woodhead Publishing; 2011, p.15. ISBN 978-0-85709-290-8.

[4] Andersson O, Semere D, Melander A, Arvidsson M, Lindberg B (2016) Digitalization of process planning of spot welding in bodyin-white. Procedia CIRP 50:618–623. https://doi.org/10.1016/j.procir.2016.05.082.

[5] Kim IS, Son JS, Kim IG, Kim JY, Kim OS (2003) A study on relationship between process variables and bead penetration for robotic CO2 arc welding. J Mater Process Technol 136:139– 145. https://doi.org/10.1016/S0924-0136(02)01126-3.

[6] Ghosal S, Chaki S (2010) Estimation and optimization of depth of penetration in hybrid CO 2 LASER-MIG welding using ANN-optimization hybrid model. Int J Adv Manuf Technol 47:1149– 1157. https://doi.org/10.1007/s00170-009-2234-1.

[7] Cheon J, Kiran DV, Na S (2016) CFD based visualization of the finger shaped evolution in the gas metal arc welding process. Int J Heat Mass Transf 97:1–14. https://doi.org/10.1016/j.ijheatmasstransfer.2016.01.067.

[8] DOWLING NE. Mechanical behavior of materials: engineering methods for deformation fracture and fatigue. 2007. ISBN 13: 978-0-273-76455-7.

[9] Kim WS, Lotsberg I. Fatigue test data for welded connections in ship-shaped structures. Journal of Offshore Mechanics and Arctic Engineering 2005;127:359–65. https://doi.org/10.1115/1.2087507.

[10] EN 1993-1-9: Eurocode 3: Design of steel structures - Part 1-9: Fatigue. 2005.

[11] EN 13001-3-1, Cranes, General design, Part 3-1: Limit States and proof competence of steel structure, 2015.

[12] Hobbacher AF. IIW Collection Recommendations for Fatigue Design of Welded Joints and Components. ISBN 978-3-319-23756-5.

[13] Xiao ZG, Yamada K. A method of determining geometric stress for fatigue strength evaluation of steel welded joints. Int J Fatigue 2004;26:1277–93. https://doi.org/10.1016/j.ijfatigue.2004.05.001.

[14] Taylor D. The theory of critical distances. Eng Fract Mech 2008;75:1696–705. https://doi.org/10.1016/j.engfracmech.2007.04.007.

[15] Neuber H (1958) Kerbspannungslehre, 2nd edn. Springer Verlag, Berlin.

[16] Dong Y, Garbatov Y, Guedes Soares C. Improved effective notch strain approach for fatigue reliability assessment of load-carrying fillet welded cruciform joints in low and high cycle fatigue. Marine Structures 2021;75:102849. https://doi.org/10.1016/j.marstruc.2020.102849.

[17] Barsoum Z, Jonsson B. Fatigue assessment and lefm analysis of cruciform joints fabricated with different welding processes. Weld World 2008;52. https://doi.org/10.1007/BF03266657.

[18] Hultgren G, Myrén L, Barsoum Z, Mansour R. Digital scanning of welds and influence of sampling resolution on the predicted fatigue performance: modelling, experiment and simulation. Metals (Basel) 2021;11:822. https://doi.org/10.3390/met11050822.

[19] Balasubramanian V, Guha B. Influence of weld size on fatigue life prediction for flux cored arc welded cruciform joints containing lack of penetration defects. Sci Technol Weld Join 2000;5:99–104. https://doi.org/10.1179/136217100101538083.

[20] Sandberg D, Mansour R, Olsson M. Fatigue probability assessment including aleatory and epistemic uncertainty with application to gas turbine compressor blades. Int J Fatigue 2017;95:132–42. https://doi.org/10.1016/j.ijfatigue.2016.10.001.

[21] Baik, Biehn, Kentaro Yamada, and Toshiyuki Ishikawa. “Fatigue strength of fillet welded joint subjected to plate bending.” International Journal of Steel Structures 8.3 (2008): 163-169.

[22] Baik B, Yamada K, Ishikawa T. Fatigue crack propagation analysis for welded joint subjected to bending. Int J Fatigue 2011;33:746–58. https://doi.org/10.1016/j.ijfatigue.2010.12.002.

[23] Xiao ZG, Chen T, Zhao XL. Fatigue strength evaluation of transverse fillet welded joints subjected to bending loads. Int J Fatigue 2012;38:57–64. https://doi.org/10.1016/j.ijfatigue.2011.11.013.

[24] Barsoum Z, Ghanadi M, Balawi S. Managing Welding Induced Distortion - Comparison of Different Computational Approaches. Procedia Eng 2015;114:70–7. https://doi.org/10.1016/j.proeng.2015.08.043.

[25] Bhatti AA, Barsoum Z, Murakawa H, Barsoum I. Influence of thermo-mechanical material properties of different steel grades on welding residual stresses and angular distortion. Mater Des 2015;65:878–89. https://doi.org/10.1016/j.matdes.2014.10.019.

[26] Teng TL, Fung CP, Chang PH, Yang WC. Analysis of residual stresses and distortions in T-joint fillet welds. Int J Press Vessel Pip 2001;78:523–38. https://doi.org/ 10.1016/S0308-0161(01)00074-6.

[27] Gharib AR, Biglari FR, Shafaie M, Kokabi AH. Experimental and numerical investigation of fixture time on distortion of welded part. Int J Adv Manuf Technol 2019;104:1121–31. https://doi.org/10.1007/s00170-019-03874-0.

[28] Yuan MG, Ueda Y. Prediction of residual stresses in welded T- and I-joints using inherent strains. J Eng Mater Technol Trans ASME 1996;118:229–34. https://doi.org/10.1115/1.2804892.

[29] Hill MR, Nelson D V. Inherent strain method for residual stress determination and its application to a long welded joint. Am Soc Mech Eng Press Vessel Pip Div PVP 1995;318:343–52.

[30] Liang X, Chen Q, Cheng L, Hayduke D, To AC. Modified inherent strain method for efficient prediction of residual deformation in direct metal laser sintered components. Comput Mech 2019;64:1719–33. https://doi.org/10.1007/s00466-019-01748-6.

[31] Souloumiac B, Boitout F, Bergheau JM (2002) A new local-global approach for the modelling of welded steel component distortions. Math Model Weld Phenom 6:573–590.

[32] Zhu J, Khurshid M, Barsoum I, Barsoum Z. Computational weld-mechanics assessment of welding distortions in a large beam structure. Eng Struct 2021;236:112055. https://doi.org/10.1016/j.engstruct.2021.112055.

[33] Tsirkas SA, Papanikos P, Pericleous K, Strusevich N, Boitout F, Bergheau JM (2003) Evaluation of distortions in laser welded shipbuilding parts using local-global finite element approach. Sci Technol Weld Join 8(2):79–88.

[34] Duan YG, Vincent Y, Boitout F, Leblond JB, Bergheau JM (2007) Prediction of welding residual distortions of large structures using a local/global approach. J Mech Sci Technol 21(10):1700–1706. https://doi.org/10.1007/BF03177397.

[35] Zhu J, Khurshid M, Barsoum Z. Accuracy of computational welding mechanics methods for estimation of angular distortion and residual stresses. Welding in the World 2019;63:1391–405. https://doi.org/10.1007/s40194-019-00746-9.

[36] Bachorski A, Painter MJ, Smailes AJ, Wahab MA. Finite-element prediction of distortion during gas metal arc welding using the shrinkage volume approach. J Mater Process Technol 1999;92–93:405–9. https://doi.org/10.1016/S0924-0136(99)00161-2.

[37] Sulaiman MS, Manurung YHP, Haruman E, Rahim MRA, Redza MR, Lidam RNA, et al. Simulation and experimental study on distortion of butt and T-joints

using WELD PLANNER. J Mech Sci Technol 2011;25:2641–6. https://doi.org/10.1007/s12206-011-0701-8.

[38] Jackson K, Darlington R. Advanced engineering methods for assessing welding distortion in aero-engine assemblies. IOP Conf Ser Mater Sci Eng 2011;26. https://doi.org/10.1088/1757-899X/26/1/012018.

[39] Dong WC, Lu SP, Lu H, Li DZ, Rong LJ, Li YY. Numerical simulation and control of welding distortion for double floor structure of high speed train. Acta Mech Sin Xuebao 2014;30:849–60. https://doi.org/10.1007/s10409-014-0108-8.

[40] Macdonald, Kenneth, ed. Fracture and fatigue of welded joints and structures. Elsevier, 2011. ISBN 978-84569-513-2.

[41] Leggatt, R. H. "Residual stresses in welded structures." International Journal of Pressure Vessels and Piping 85.3 (2008): 144-151. https://doi.org/10.1016/j.ijpvp.2007.10.004.

[42] Kohandehghan, A. R., and S. Serajzadeh. "Arc welding induced residual stress in butt-joints of thin plates under constraints." Journal of manufacturing processes 13.2 (2011): 96-103. https://doi.org/10.1016/j.jmapro.2011.01.002.

[43] Wang, Yifeng, et al. "Influence of welding sequence on residual stress distribution and deformation in Q345 steel H-section butt-welded joint." Journal of Materials Research and Technology 13 (2021): 144-153. https://doi.org/10.1016/j.jmrt.2021.04.059.

[44] Akbari, D., and I. Sattari-Far. "Effect of the welding heat input on residual stresses in butt-welds of dissimilar pipe joints." International journal of pressure vessels and piping 86.11 (2009): 769-776. https://doi.org/10.1016/j.ijpvp.2009.07.005.

[45] Yang, Y.P., Brust, F.W. and Kennedy, J.C., 2002, January. Lump-pass welding simulation technology development for shipbuilding applications. In ASME 2002 Pressure Vessels and Piping Conference (pp. 47-54). American Society of Mechanical Engineers. https://doi.org/10.1115/PVP2002-1105.

[46] Liu C, Luo Y, Yang M, Fu Q. Three-dimensional finite element simulation of welding residual stress in RPV with two J-groove welds. Welding in the World 2017;61:151–60. https://doi.org/10.1007/s40194-016-0392-y.

[47] Zhu J, Khurshid M, Barsoum Z. Assessment of computational weld mechanics concepts for estimation of residual stresses in welded box structures. Procedia Structural Integrity 2019;17:704–11. https://doi.org/10.1016/j.prostr.2019.08.094.

[48] Hu X, Feng G, Wang Y, Zhang C, Deng D. Influence of lumping passes on calculation accuracy and efficiency of welding residual stress of thick-plate butt joint in boiling water reactor. Eng Struct 2020;222:111136. https://doi.org/10.1016/j.engstruct.2020.111136.

[49] Malmelöv, A.; Lundbäck, A.; Lindgren, L.-E. History Reduction by Lumping for Time-Efficient Simulation of Additive Manufacturing. Metals 2020, 10, 58. https://doi.org/10.3390/met10010058.

[50] Goldak, J., Chakravarti, A. and Bibby, M., 1984. A new finite element model for welding heat sources. Metallurgical transactions B, 15(2), pp.299- 305. https://doi.org/10.1007/BF02667333.

[51] Lindgren, L.E., Runnemalm, H. and Näsström, M.O., 1999. Simulation of multipass welding of a thick plate. International journal for numerical methods in engineering, 44(9), pp.1301-1316. https://doi.org/10.1002/(SICI)1097-0207(19990330)44:9<1301::AID-NME479>3.0.CO;2-K.

[52] Suban M, Tusek J (2003) Methods for the determination of arc stability. J Mater Process Technol 143:430–7. https://doi.org/10.1016/S0924-0136(03)00416-3.

[53] Kim JW, Na SJ (1991) A study on prediction of welding current in gas metal arc welding part 1: modelling of welding current in response to change of tip-to-workpiece distance. Proc Institut Mech Eng Part B: J Eng Manuf 205:59–63. https://doi.org/10.1243/PIME_PROC_1991_205_051_02.

[54] Mansour R, Zhu J, Edgren M, Barsoum Z. A probabilistic model of weld penetration depth based on process parameters. International Journal of Advanced Manufacturing Technology 2019;105:499–514. https://doi.org/10.1007/s00170-019-04110-5.

[55] Cochran, W. G. (1977). Sampling techniques. John Wiley & Sons.

[56] Poutiainen I, Tanskanen P, Marquis G. Finite element methods for structural hot spot stress determination - A comparison of procedures. Int J Fatigue 2004;26:1147–57. https://doi.org/10.1016/j.ijfatigue.2004.04.003.

[57] Taylor D. The Theory of Critical Distances. 2007. ISBN: 9780080554723.

[58] Baumgartner J, Schmidt H, Ince E, Melz T, Dilger K. Fatigue assessment of welded joints using stress averaging and critical distance approaches. Welding in the World 2015;59:731–42. https://doi.org/10.1007/s40194-015-0248-x.

[59] Sonsino CM, Fricke W, de Bruyne F, Hoppe A, Ahmadi A, Zhang G. Notch stress concepts for the fatigue assessment of welded joints - Background and applications. Int J Fatigue 2012;34:2–16. https://doi.org/10.1016/j.ijfatigue.2010.04.011.

[60] Neuber, Heinz. "Über die Berücksichtigung der spannungskonzentration bei festigkeitsberechnungen." Konstruktion 20.7 (1968): 245-251.

[61] Karakaş Ö. Application of Neuber's effective stress method for the evaluation of the fatigue behaviour of magnesium welds. Int J Fatigue 2017;101:115–26. https://doi.org/10.1016/j.ijfatigue.2016.10.023.

[62] Radaj D. Design and analysis of fatigue resistant welded structures. Cambridge: Abington Publishing; 1990. ISBN 1 85573 004 9.

[63] Sonsino, Cetin Morris. "A consideration of allowable equivalent stresses for fatigue design of welded joints according to the notch stress concept with the reference radii r ref= 1.00 and 0.05 mm." Welding in the World 53.3 (2009): R64-R75. https://doi.org/10.1007/BF03266705.

[64] Schijve J. Fatigue predictions of welded joints and the effective notch stress concept. Int J Fatigue 2012;45. https://doi.org/10.1016/j.ijfatigue.2012.06.016.

[65] Fitria. Fricke, Wolfgang. IIW recommendations for the fatigue assessment of welded structures by notch stress analysis: IIW-2006-09. Woodhead Publishing, 2012.

[66] Fricke W, Kahl A. Local stress analysis and fatigue assessment of bracket toes based on measured weld profile. International Institute of Welding 2007. IIW-doc. XIII-2166-07/XV-1253-07.

[67] Pedersen MM, Mouritsen OO, Hansen MR, Andersen JG, Wenderby J. Re-analysis of fatigue data for welded joints using the notch stress approach. Int J Fatigue 2010;32. https://doi.org/10.1016/j.ijfatigue.2010.03.001.

[68] Rohani Raftar H, Dabiri M, Ahola A, Björk T. Re-evaluation of weld root fatigue strength for load-carrying fillet welded joints using the notch stress concept. Int J Fatigue 2021;144. https://doi.org/10.1016/j.ijfatigue.2020.106076.

Appended Papers